

18. Cooke C, Garcia E, Cullom S, Faber T, Pettigrew R. Determining the accuracy of calculating systolic wall thickening using a fast Fourier transform approximation: a simulation study based on canine and patient data. *J Nucl Med* 1994;35:1185–1192.
19. Bland J, Altman D. Statistical methods for assessing agreement between two methods of clinical measurement. *Lancet* 1986;1:307–310.
20. Fleiss J. *Statistical methods for rates and proportions*, 2nd ed. New York, NY: Wiley; 1981.
21. Mazzanti M, Germano G, Kiat H, et al. Identification of severe and extensive coronary artery disease by automatic measurement of transient ischemic dilation of the left ventricle in dual-isotope myocardial perfusion SPECT. *J Am Coll Cardiol* 1996;27:1612–1620.
22. Weiss A, Berman D, Lew A, et al. Transient ischemic dilation of the left ventricle on stress thallium-201 scintigraphy: a marker of severe and extensive coronary artery disease. *J Am Coll Cardiol* 1987;9:752–759.

# Comparison of SPECT and Ectomography for Evaluating Myocardial Perfusion with Technetium-99m-Sestamibi

Susanne M. Dale, Dianna E. Bone, Lars-Åke Brodin and Catharina Lindström

Department of Medical Laboratory Sciences and Technology, Division of Medical Engineering, Karolinska Institute;  
Department of Clinical Physiology, Thoracic Clinics, Karolinska Hospital, Huddinge, Sweden

This study compared myocardial perfusion scintigraphy performed with ectomography to corresponding SPECT studies. **Methods:** In a comparative study between SPECT and ectomography, 19 patients with suspected coronary artery disease were imaged under similar conditions. A two-day protocol using  $^{99m}\text{Tc}$ -sestamibi was followed. In SPECT, 32 projection images were acquired by rotating the gamma camera detector through  $180^\circ$ , from  $45^\circ$  left posterior oblique to  $45^\circ$  right anterior oblique. Short-axis view sections and polar tomograms were reconstructed. In ectomography, a  $30^\circ$  slant-hole collimator was rotated through  $360^\circ$  in front of a stationary detector to obtain 64 projection images with different projection directions. The gamma camera was orientated perpendicular to the long axis of the left ventricle; the orientation was determined from the SPECT examination. Short-axis section images through the projected conical volume were reconstructed using a two-dimensional filtered back projection technique. In a blind test, the relative diagnostic value and image quality of the two methods were evaluated by three independent observers assessing short-axis view sections and polar tomograms. An objective evaluation based on relative values in the polar tomograms was also performed. The interpretations were evaluated with analysis of variance. **Results:** After injection during exercise, there was no significant difference between SPECT and ectomography. After injection at rest, visualization of the left ventricle was superior ( $p < 0.05$ ) and influence of external activity was less ( $p < 0.005$ ) in ectomography. The activity level within a perfusion defect was significantly lower ( $p < 0.05$ ) and its extension significantly larger ( $p < 0.05$ ) in ectomography than in SPECT. There was no difference between the diagnosis based on SPECT or ectomography. **Conclusion:** In myocardial perfusion imaging with  $^{99m}\text{Tc}$ -sestamibi, ectomography provides information similar to that obtained with SPECT and can, therefore, be used clinically for evaluation of myocardial perfusion when the gamma camera is positioned perpendicular to the long axis of the left ventricle.

**Key Words:** coronary artery disease; myocardial perfusion; SPECT; technetium-99m-sestamibi; ectomography

*J Nucl Med* 1997; 38:754–759

**M**yocardial perfusion imaging for diagnosis of coronary artery disease is generally performed using SPECT. A gamma camera detector is rotated around the long axis of the patient, consequently a SPECT system is heavy and stationary. The distance to the object imaged is, for most projection images, rather large, reducing resolution and increasing the attenuation

effects. Since a patient must be transported to the camera and is required to lie on a narrow examination table, it is difficult or impossible to perform examinations on critically ill patients connected to life support equipment, such as a ventilator, aortic balloon pump or extra corporeal membrane oxygenation (ECMO) machine. Furthermore, it has been shown that myocardial perfusion scintigraphy provides both diagnostic and prognostic information in patients with suspected acute myocardial infarction (1–5). It would, therefore, assist in patient management if such studies could be performed at the bedside, or in the emergency room on patients presenting chest pain.

A tomographic method called ectomography has been developed and implemented in gamma camera imaging (6). Ectomography is a limited-view angle method and a set of projection images can be obtained by rotating a slant-hole collimator in front of a stationary gamma camera detector. No complex, heavy gantry for the rotation of the camera is required, making the technique suitable for implementation in a mobile system. Mobility provides the possibility of tomographic imaging in almost all hospital environments, for example in the intensive care unit, emergency room or in the operating theater. Since no active patient cooperation is required, both seriously ill and unconscious patients can be studied. Another advantage of the technique is that the detector can be positioned close to the object during the acquisition of all projection images, thus increasing resolution and reducing attenuation effects. All limited-view angle methods are characterized, however, by an incomplete dataset. For ectomography, this leads to a reduction in depth resolution, which is inversely dependant on view angle (7). With the current reconstruction technique, only slices perpendicular to the axis of rotation are tenable. In an extended object, this effect can be minimized by positioning the long axis of the object along the axis about which the collimator rotates (alt axis of rotation). Thus, when imaging the left ventricle, short-axis view slices are obtained when positioning is optimized.

Ectomography has previously been evaluated by computer simulations, phantom studies and a limited number of clinical examinations (8–9). A first prototype mobile system was designed and built in our department and is currently at the Department of Clinical Physiology, Thoracic Clinics, Karolinska Hospital, for preliminary clinical evaluation (10–12).

This is a comparative study between SPECT and ectomography to verify the clinical accuracy of ectomography for myocardial perfusion imaging using  $^{99m}\text{Tc}$ -sestamibi under ideal geometrical conditions. Thus, to avoid the possible effects

Received Apr. 1, 1996; revision accepted Oct. 2, 1996.

For correspondence or reprints contact: Susanne Dale, PhD, Division of Medical Engineering, F60, Novum, S-141 86 Huddinge, Sweden.

**TABLE 1**

Acquisition and Reconstruction Parameters for SPECT and Ectomography

	SPECT	Ectomography
Number of projections	32	64
Time per projection	30 sec	20 sec
Rotational mode	180°	360°
Pixel size	5 mm	6.25 mm
Matrix size	64 × 64	64 × 64
Prefiltering	Metz filter	No
Reconstruction filter	Ramp	Modified Shepp-Logan
Attenuation correction	Yes	No

of mispositioning, the orientation of the left ventricle was obtained from the SPECT examination by studying short-axis view images obtained from the two modalities.

## MATERIALS AND METHODS

Nineteen consecutive patients (nine men, 10 women; age range 38–73 yr, mean 57.2 yr ± 9.4 yr) referred for routine SPECT myocardial imaging were studied. Informed consent was obtained.

Approximately 400 MBq  $^{99m}$ Tc-sestamibi was injected intravenously during maximum-symptom limited exercise on a bicycle ergometer. Acquisition of projection images was started 30 min after injection. Two days later, a similar amount of radiopharmaceutical was administered at rest and the acquisition procedure repeated. After the exercise injection, SPECT was performed first, immediately followed by ectomography. At rest, the ectomographic acquisition was performed before the SPECT acquisition in four of the 19 patients. Since there is very little or no redistribution of  $^{99m}$ Tc-sestamibi (13), the order of acquisition between the two methods was not relevant. Acquisition and reconstruction parameters for the two methods are presented in Table 1.

SPECT images were acquired with a gamma camera equipped with a low-energy, general purpose, parallel-hole collimator. The detector was rotated from 45° LPO to 45° RAO and 32 projection images were acquired.

In ectomography, a stationary gamma camera system fitted with a rotating 30° slant-hole collimator (low-energy, general purpose) was used. The collimator was rotated manually through 360° and 64 projection images were obtained. The gamma camera detector was orientated perpendicular to the long axis of the left ventricle; the orientation was determined from the SPECT examination. In

**TABLE 2**

Ratings Used to Assess Image Quality and Relative Diagnostic Value of SPECT and Ectomography

Evaluated parameter	Ratings
Image quality	3 = excellent, 2 = very good, 1 = good, 0 = poor
Visualization of left ventricle (definition of cavity and walls, contrast, external activity)	3 = excellent, 2 = very good, 1 = good, 0 = poor
Visualization of right ventricle (definition of cavity and walls, contrast, external activity)	3 = excellent, 2 = very good, 1 = good, 0 = poor
Influence of external activity	3 = disturbing to a great extent, 2 = to some extent, 1 = slightly, 0 = not at all disturbing
Activity level in defect	4 = 100%, 3 = > 75%, 2 = 50%–75%, 1 = 25%–50%, 0 = < 25%
Extent of perfusion defect	3 = large, 2 = medium, 1 = small, 0 = none
Probability of coronary disease	4 = high, 3 = medium, 2 = low, 1 = none, 0 = inconclusive
Probability of infarction	4 = high, 3 = medium, 2 = low, 1 = none, 0 = inconclusive

Figure 1, the acquisition geometries for SPECT and ectomography are shown.

Evaluation of myocardial perfusion was made from reconstructed short-axis section images and polar tomograms. The nominal thickness of short-axis section images was 10 mm for SPECT and 12 mm for ectomography. The reconstruction filter in ectomography was chosen to produce images resembling the SPECT images in appearance. In SPECT, linear attenuation correction was performed (14).

A subjective assessment of imaging results was made by three experienced observers (a clinical cardiologist, a nuclear cardiologist and a radiologist accustomed to interpreting myocardial scintigrams), who evaluated two sets of reconstructed short-axis section images and polar tomograms in a blind test, according to the criteria given in Table 2. The two sets of images were compared, both with regard to image quality and diagnostic information. One image consisted of the short-axis view sections

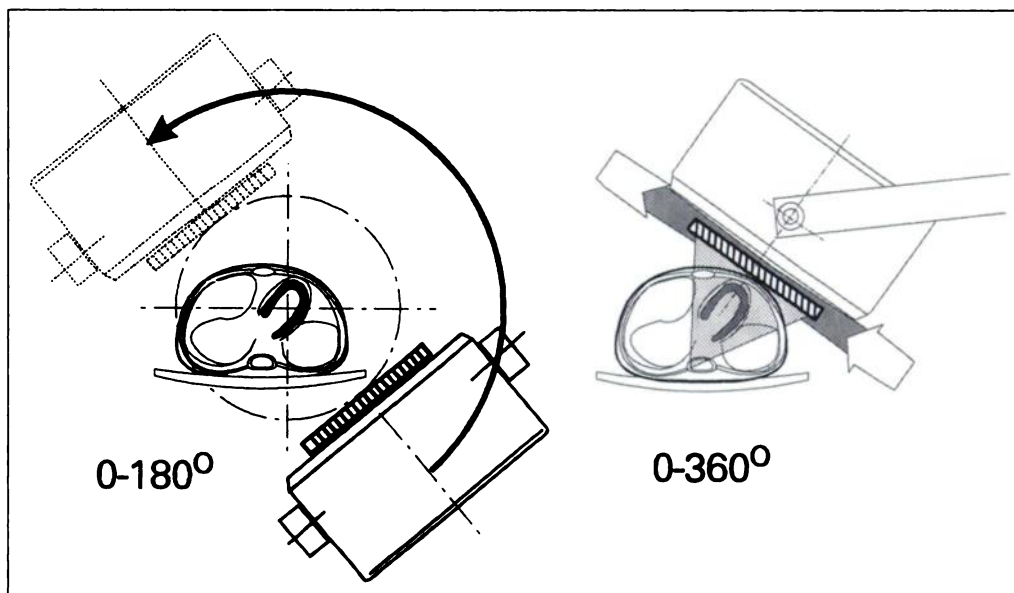


**FIGURE 1.** Acquisition geometries for (left) SPECT and (right) ectomography, respectively, for tomographic myocardial perfusion imaging.

TABLE 3

Summary of Results from an Analysis of Variance of Data Obtained from Three Independent Observers Evaluating the Individual Images (Image Set One)

Exercise	SPECT versus ectomography
Image quality	ns
Visualization of left ventricle	ns
Influence of external activity	ns
Visualization of right ventricle	ns
Existence of perfusion defect	ns
Activity level in defect	ns
Extent of perfusion defect	ns
Rest	
Image quality	ns
Visualization of left ventricle	p < 0.05*
Influence of external activity	p < 0.005†
Visualization of right ventricle	ns
Existence of perfusion defect	ns
Activity level in defect*	p < 0.05‡
Extent of perfusion defect*	ns

\*SPECT: 1.46 ± 0.85; ectomography: 1.82 ± 0.70

†SPECT: 1.61 ± 0.89; ectomography: 1.17 ± 0.85

‡SPECT: 3.44 ± 1.09; ectomography: 3.15 ± 1.27

ns = no significant difference.

TABLE 4

Summary of Results from an Analysis of Variance of Data Obtained from Three Independent Observers Evaluating the Complete Patient Studies (Image Set Two)

Exercise	SPECT versus ectomography
Existence of perfusion defect	ns
Activity level in defect	ns
Extent of perfusion defect	ns
Rest	
Existence of perfusion defect	ns
Activity level in defect	ns
Extent of perfusion defect	p < 0.05*
Probability of coronary artery disease	ns
Probability of infarction	ns

\*SPECT: 0.25 ± 0.55; ectomography: 0.61 ± 0.94

ns = no significant difference.

## RESULTS

### Set 1

*Comparison of Individual Acquisitions.* After injection during maximum exercise, there was no significant difference ( $p < 0.05$ ) between SPECT and ectomography regarding image quality. The results of the variance analysis of image Set 1 are summarized in Table 3. There was no difference in interpretation of the presence of a perfusion defect, position of a detected perfusion defect, level of activity in the central part of the defect or its extent. After injection at rest, ectomography resulted in a significantly better visualization of left ventricle with regard to definition of the cavity and walls, contrast and external activity than SPECT (1.82 ± 0.70 versus 1.46 ± 0.85,  $p < 0.05$ ) and the influence of external activity was less (1.17 ± 0.85 versus 1.61 ± 0.89,  $p < 0.005$ ). The activity level within a defect was significantly lower in ectomography than in SPECT (3.15 ± 1.27 versus 3.44 ± 1.09,  $p < 0.05$ ), but there was no difference in the extent of the defect.

For both exercise and rest data, intraobserver reproducibility was good. However, there was a significant difference between observers in the estimation of image quality and the existence of a perfusion defect, but not in estimation of defect activity or extension.

### Set 2

*Comparison of Complete Patient Studies.* After injection during maximum exercise, there was no difference between SPECT and ectomography regarding the presence of a perfusion defect, its activity level or extent. However, after injection at rest there was a significant difference in the estimation of the extent of the defect (0.61 ± 0.94 for ectomography versus 0.25 ± 0.55 for SPECT,  $p < 0.05$ , with 0 being no extent and 1 small extent), but not in the activity level. For diagnosis, that is the probability of coronary artery disease and myocardial infarction, there was no difference between the two methods. There was a significant difference between observers in the estimation of central activity within a defect and its extent after the exercise injection and also in the diagnosis of the probability of coronary artery disease. The results are summarized in Table 4.

*Objective Evaluation.* There were no significant differences between SPECT and ectomography in the objective evaluation of exercise and rest data, either in activity level within a perfusion defect or in the size of the perfusion defect. To illustrate the similarities and differences in reconstructed sec-

and the generated polar tomogram. In set one, an image consisted of short-axis section images and the corresponding polar tomogram from one acquisition, either exercise or rest. Observers rated, on a four-point scale, overall image quality, visualization of left and right ventricle regarding definition of the cavity and walls, contrast and external activity, influence of activity outside the myocardium and the extent of a perfusion defect for each coronary artery. On a five-point scale, the level of activity in the perfusion defect for each coronary artery and the probability of coronary artery disease or infarction was rated. Each image was presented twice to allow estimation of intraobserver variability. Set 1 consisted of 100 images. In the second set, one image consisted of short-axis view sections and the generated polar tomograms from the complete patient study (exercise and rest). Set 2 comprised eight patients and was assessed with respect to diagnostic information.

Results from the first set were analyzed using four-factor analysis of variance on the exercise and rest data, respectively. The results of the second set were analyzed using a three-factor analysis of variance also separated into exercise and rest.

An objective evaluation based on relative values in the polar tomograms was also performed. For each coronary artery, the activity level in a perfusion defect was determined according to the same scale as used by the observers with the condition that at least 10% of the pixels in the region were within the specified range. The size of a perfusion defect was quantified as the percentage of pixels in each region less than 60% of the maximum value in the polar tomogram (15). The evaluation showed that 0%–10% of such pixels in the polar tomograms were graded as none, 10%–35% as small, 35%–60% as medium and > 60% as large. The position and extent of the region supplied by each coronary artery were chosen in accordance with Svane (16).

All results are presented as mean ± 1 s.d. Analysis of variance was performed using the Statistical Package for the Social Sciences (SPSS) for Microsoft Windows release 6.1. Results were significant if  $p < 0.05$ .

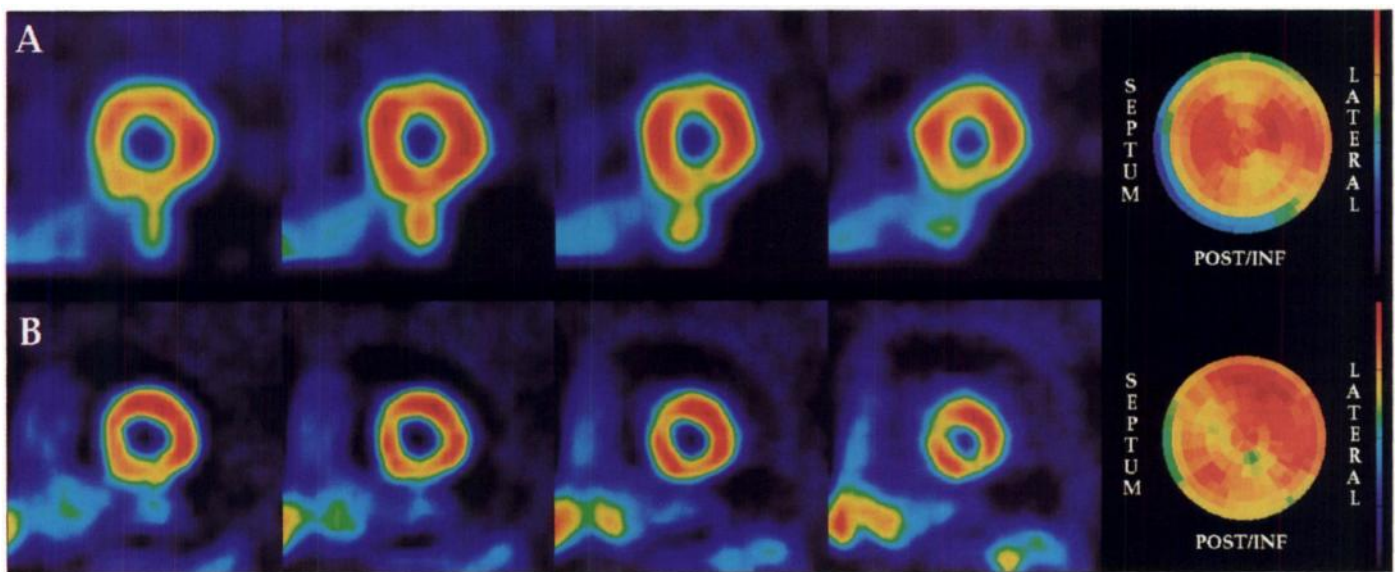


**FIGURE 2.** Reconstructed SPECT (A) and ectomography section images (B) after injection at rest of a 63-yr-old healthy man with no perfusion defects. Shown are reconstructed short-axis section images, basal-to-apical of 10-mm and 12-mm thicknesses and polar tomograms for the two methods.

tion images and generated polar tomograms between SPECT and ectomography, three patient studies are presented.

Figure 2 shows reconstructed section images with SPECT and ectomography after injection at rest from a 63-yr-old man. Since the pixel size and section thickness for the two methods differ slightly, section images cannot be exactly compared. The short-axis view sections and polar tomograms of the two sets of images are very similar. The images show uniform perfusion of the myocardium, without significant perfusion defects.

Figure 3 shows reconstructed section images from SPECT and ectomography in a 73-yr-old man after injection at rest. The images show a large perfusion defect in the anterior wall of the myocardium and a small defect in the posterior wall. The position and extent of the perfusion defect are approximately the same for the two methods. In ectomography, the right ventricle is visible. Due to the high uptake of the isotope in the liver, interpretation of the perfusion in the posterior wall is difficult in SPECT. With ectomography, the separation between

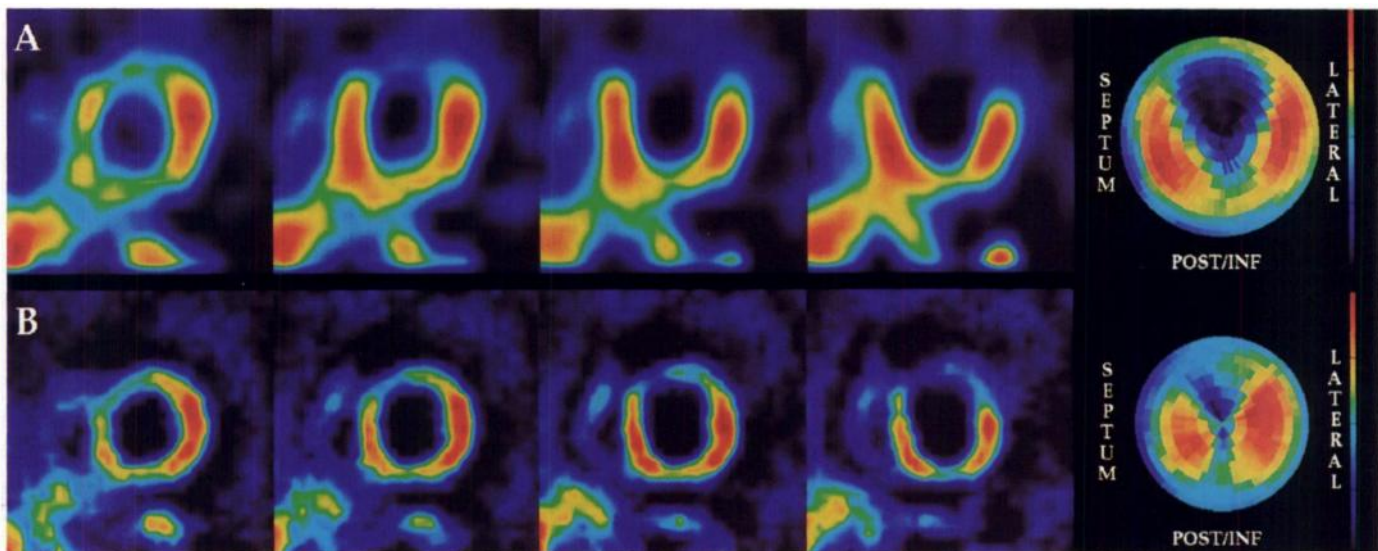
the liver and the myocardium is better, giving a better estimation of perfusion in the posterior wall of the myocardium.

Figure 4 shows reconstructed section images with SPECT and ectomography from a 52-yr-old man after injection at rest. The images show a perfusion defect in the posterior wall of the myocardium. The position and extent of the perfusion defect are approximately the same for the two methods.

## DISCUSSION

In this comparative study of 19 patients with suspected coronary artery disease, SPECT and ectomography appear to have the same diagnostic value for evaluation of myocardial perfusion and diagnosis of coronary artery disease using  $^{99m}\text{Tc}$ -sestamibi when alignment of the left ventricular long axis is used.

Since ectomography is a limited-view angle method in which the total angle subtended by the projection images is less than the minimum  $180^\circ$  required for a correct reconstruction (7), the



**FIGURE 3.** Reconstructed SPECT (A) and ectomography section images (B) after injection during exercise of a 73-yr-old man with a large perfusion defect in the anterior wall. Shown are reconstructed short-axis section images, basal-to-apical of 10-mm and 12-mm thicknesses and polar tomograms for the two methods.

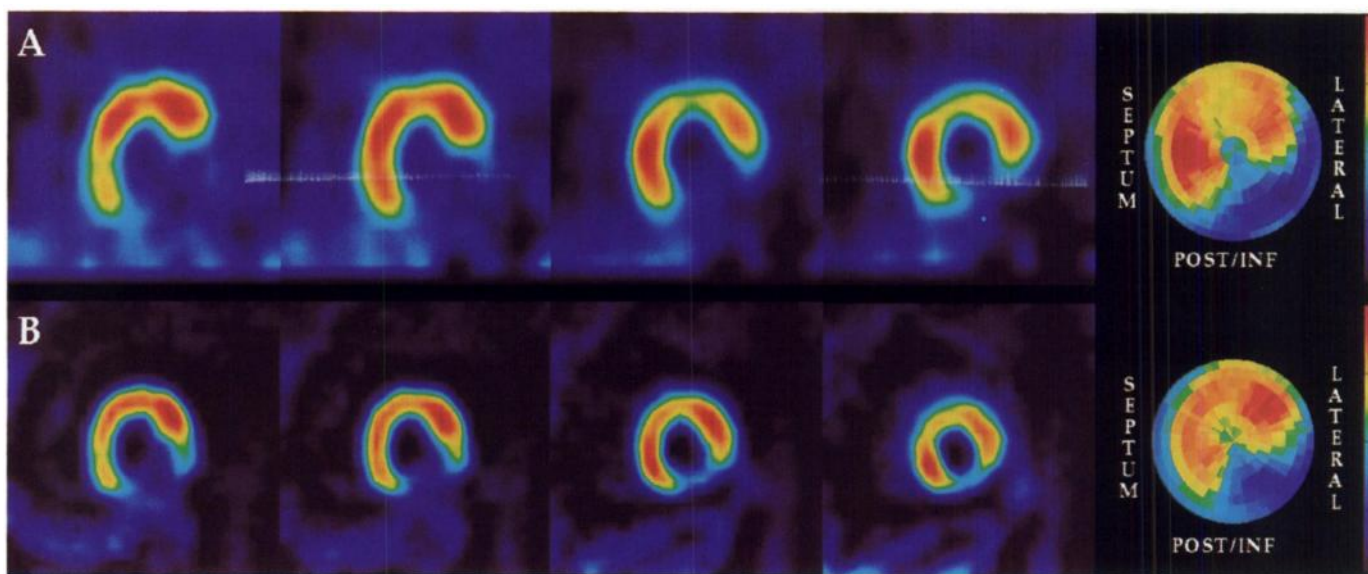


**FIGURE 4.** Reconstructed SPECT (A) and ectomography (B) section images after injection at rest of a 52-yr-old man with a large perfusion defect in the posterior wall. Shown are reconstructed short-axis section images, basal to apical of 10-mm and 12-mm thicknesses and polar tomograms for the two methods.

reconstruction problem is undetermined, and no unique solution for the source distribution can be given. In practice, this results in the propagation of reconstructed activity distribution from one section image into adjacent ones and consequently reduced depth resolution. In an extended object, such as the left ventricular myocardium, ideal orientation of the gamma camera is obtained when the axis of rotation and long axis of the left ventricle coincide. The prime object of this initial comparative study was, however, to compare true short-axis images from SPECT and ectomographic studies without the additional problem of differences in orientation. Therefore, the gamma camera was positioned according to the long-axis orientation determined from the corresponding SPECT study, for the ectomographic examination.

The reason for the perpendicular orientation of the camera with respect to the left ventricular long axis is that limited-view angle methods are characterized by an incomplete set of Fourier coefficients of the object imaged due to the projection procedure described above. The missing coefficients in the Fourier domain represent a volume shaped as a double cone that has an axis of symmetry parallel to the axis of rotation during the projection procedure. The missing cone results in limited resolution in the depth direction and causes propagation of reconstructed activity distribution from one section image into adjacent ones. To minimize this effect in myocardial imaging, therefore, the gamma camera detector should be oriented perpendicular to the long axis of the left ventricle. This requires a priori knowledge of the orientation of the myocardium within the thorax, or the possibility of determining this from the projection images before the start of acquisition.

In this comparative study, the orientation obtained from the SPECT acquisition was used to position the gamma camera for the ectomographic acquisition in order to eliminate differences that could be due to poor camera positioning. In a previous limited clinical study (9), the gamma camera was oriented in a left anterior oblique 30° position with a 15° cranial tilt for all patients, thus disregarding the true orientation of the myocardium. Only one of these studies could not be reconstructed successfully. The mean misalignment of the camera with respect to the long axis of the left ventricle as determined from the SPECT acquisition, was +7° in the left anterior oblique

direction and +4° in the cranial direction. Hence, by positioning the gamma camera with an orientation of left anterior oblique 35° with a 15–20° cranial tilt, alignment within ± 10° can be achieved for most patients. The effects of misalignment have been evaluated with phantom studies using  $^{201}\text{TI}$  (9), which show that the effects are dependent on the position of the section and are most pronounced in basal section images. Work is, however, currently in progress to enable determination of the orientation of the myocardium from a set of projection images.

This comparative study shows that when perfusion defects are present in the short-axis section images obtained after injection during exercise, their position, extent and severity are in agreement between the two methods. The diagnosis of coronary artery disease and/or myocardial infarction is the same as for SPECT. In the objective evaluation based on relative pixel values in the polar tomograms, there was no significant difference between the methods.

In the subjective assessment after injection at rest, however, there are differences between the methods. The visualization of the left ventricle is superior in ectomography, which is probably due to the more favorable acquisition geometry. When the gamma camera detector is positioned in a direction perpendicular to the long axis of the left ventricle, the myocardium is within 5–20 cm of the detector surface. In this region volume resolution is superior in ectomography compared to SPECT (8) and this could explain the better separation of the walls of the ventricle and the cavity and the improved image quality.

There were also differences between SPECT and ectomography in the subjective assessment of the activity level in the central part of a perfusion defect in the set comprising individual rest acquisitions (Set 1) and the extent of a perfusion defect in the set comprising complete studies (Set 2). The activity level is lower and the extent larger with ectomography, especially in the inferior wall of the myocardium. Short-axis view sections and the corresponding polar tomogram from one patient were assessed differently when evaluated separately compared to the complete study comprising both exercise and rest data. In this patient, a significant difference in activity distribution within the liver and gastrointestinal tract was observed between the SPECT and ectomographic acquisition.

In tomographic imaging with  $^{99\text{m}}\text{Tc}$ -sestamibi, a serious

problem, especially after injection at rest, is the high uptake of the radiopharmaceutical in regions external to the myocardium, in other words, the gastrointestinal tract and liver. Organs positioned close to the heart, such as the liver, constitute the greatest problem. With SPECT acquisition geometry, these areas are projected very close to or even superimposed on the heart in some projection images leading to difficulties in evaluating perfusion in the posterior wall of the myocardium. In reconstructed section images after injection at rest, ectomography gives a significantly better separation between the liver and the myocardium and, therefore, increases the possibility of correctly determining perfusion in the posterior wall. The higher in-section resolution combined with a more favorable acquisition geometry achieved in ectomography may explain differences in activity level and extent subjectively assessed in the rest images.

Interobserver variability was greater than intermethod variability. However, the standard deviation for each observer was approximately the same, whereas the mean values were different. This indicates that the observers have slightly different references and criteria for interpreting the section images, but that the variation in their interpretations was of the same order.

Ectomography is not the only method using a gamma camera detector and rotating slant-hole collimator that has been reported for use in myocardial perfusion scintigraphy (17–26). Other methods have, however, produced relatively poor results. Ectomography differs from these methods in two fundamental aspects. The angular sampling frequency is typically eight times higher than for other methods and the current reconstruction algorithm uses a filtered backprojection technique instead of an iterative algorithm. With a low angular sampling frequency image distortion can arise if the object does not have rotational symmetry about the axis of rotation. This is the case when perfusion defects are present in the myocardium and might to some extent explain the poor results previously reported with rotating slant hole tomography. Furthermore, in many applications the slant angle of the collimator holes was less than 30°, which further reduces the depth resolution.

Depth resolution may be improved through optimization of acquisition and reconstruction parameters for myocardial perfusion studies. No optimization of the ectomographic technique was made in this study. An increased depth resolution would make it feasible to reconstruct arbitrarily oriented sections within the reconstruction volume. The gamma camera can then be positioned as close as possible to the patient independent of the orientation of the myocardium, in practice, in contact with the thorax of the patient. A shorter distance to the object also results in not only improved resolution within the imaged section, but also a higher signal-to-noise ratio due to a reduction in the effects of scatter and attenuation. The effectiveness of the system is increased making it possible to reduce acquisition times and/or injected dose.

## CONCLUSION

In this study based on 19 patients with suspected coronary artery disease, ectomography performed with the gamma camera positioned perpendicular to the long-axis of the left ventricle results in three-dimensional images of myocardial perfusion that are of the same diagnostic value as SPECT. Image quality after injection at rest is higher than in SPECT. Ectomography can be implemented on a mobile system enabling three-dimensional imaging to be performed in almost all hospital environments. A mobile tomographic system allows acute studies within the emergency room for diagnosis and early treatment of myocardial infarction as well as in the intensive

care unit for investigation of acute ischemia or infarction after coronary artery bypass surgery.

## ACKNOWLEDGMENTS

We thank Dr. Lars Grip, Professor Alf Holmgren and Dr. Bertil Svane for their help in interpreting the scintigrams.

This study was supported by grants from the Swedish Medical Research Council (project no. 10861), the Swedish Board for Industrial and Technical Development (project no. 83-04086P), the Swedish Research Council for Engineering Sciences (project no. 94-247) and the Swedish Heart and Lung Foundation and the Research and Development Fund at the Karolinska Hospital.

## REFERENCES

1. Weissman IA, Dickinson C, Dworkin H, et al. Emergency center myocardial perfusion SPECT—long-term follow-up: cost-effective imaging providing diagnostic and prognostic information [Abstract]. *J Nucl Med* 1995;36:88P.
2. Stowers SA, Abuan TH, Szymanski TJ, et al. Technetium-99m sestamibi SPECT and <sup>99m</sup>Tc-tetrofosmin SPECT in prediction of cardiac events in patients injected during chest pain and following resolution of pain [Abstract]. *J Nucl Med* 1995; 36:88–89P.
3. Hilton TC, Thompson RC, Williams HJ, Saylors R, Fulmer H, Stowers SA. Technetium-99m sestamibi myocardial perfusion imaging in the emergency room evaluation of chest pain. *J Am Coll Cardiol* 1994;23:1016–1022.
4. Varetti T, Cantalupi D, Altieri A, Orlandi C. Emergency room <sup>99m</sup>Tc-sestamibi imaging to rule out acute myocardial ischemic events in patients with nondiagnostic electrocardiograms. *J Am Coll Cardiol* 1993;22:1804–1808.
5. Brown KA. Prognostic value of thallium-201 myocardial perfusion imaging in three primary patient populations. *Am J Cardiol* 1992;70:23E–29E.
6. Dale S. Ectomography—theory and implementation in gamma camera imaging [PhD dissertation]. Stockholm, Sweden: Royal Institute of Technology; 1989.
7. Chiu MY, Barrett HH, Simpson RG, Chou C, Arendt JW, Gindi GR. Three-dimensional radiographic imaging with a restricted view angle. *J Opt Soc Am* 1979;69:1323–1333.
8. Dale SM, Bone D. Tomography using a rotating slant-hole collimator and a large number of projections. *J Nucl Med* 1990;31:1675–1681.
9. Dale SM, Bone D. Thallium-201 myocardial tomography using a rotating slant-hole collimator and a large number of projections. *J Nucl Med* 1990;31:1682–1688.
10. Dale S, Bone D, Brodin L-Å, et al. Tomographic myocardial perfusion studies in the intensive care unit using a mobile gamma camera system. *Proceedings of the American College of Cardiology 44th Annual Scientific Session*. New Orleans, LA: American College of Cardiology; 1995;192A.
11. Dale S, Bone D, Brodin L-Å, et al. Bedside tomographic myocardial perfusion imaging in the intensive care unit using a mobile gamma camera system [Abstract]. *J Nucl Cardiol* 1995;2:S34.
12. Dale S, Bone D, Brodin L-Å, et al. A mobile tomographic gamma camera system for acute studies. *IEEE Trans Nucl Sci* 1997; in press.
13. Zaret BL, Wackers FJ. Nuclear cardiology: first of two parts. *N Engl J Med* 1993;329:775–783.
14. Larsson S. Gamma camera emission computed tomography. *Acta Radiol* 1980; 363 (suppl).
15. Christian TF, Schwartz RS, Gibbons RJ. Determinants of infarct size in reperfusion therapy for acute myocardial infarction. *Circulation* 1992;86:81–90.
16. Svane B. Polar presentation of coronary angiography and thallium-201 single-photon emission computed tomography [MD dissertation]. Stockholm, Sweden: Karolinska Institute; 1990.
17. Muehllehner G. A tomographic scintillation camera. *Phys Med Biol* 1971;16:87–96.
18. Freedman GS. Tomography with a gamma camera. *J Nucl Med* 1970;11:602–604.
19. Ratib O, Henze E, Hoffman E, Phelps ME, Schelbert HR. Performance of the rotating slant-hole collimator for the detection of myocardial perfusion abnormalities. *J Nucl Med* 1982;23:34–41.
20. Chang W, Lin SL, Henkin RE. A new collimator for cardiac tomography: the quadrant slant-hole collimator. *J Nucl Med* 1982;23:830–835.
21. Mills JA, Flint J, Taylor DN, Delchar T, McIntosh JA, Pilcher J. Thallium-201 scintigraphy for ischemic heart disease and infarct detection: comparison of rotating slant-hole tomography and planar imaging. *Br J Radiology* 1985;58:625–634.
22. Starling MR, Dehmer GJ, Lancaster JL, et al. Segmental coronary artery disease: detection by rotating slant-hole collimator tomography and planar thallium-201 myocardial scintigraphy. *Radiology* 1985;157:231–237.
23. Lancaster JL, Starling MR, Kopp DT, Lasher JC, Blumhardt R. Effect of errors in reangulation on planar and tomographic thallium-201 washout profile curves. *J Nucl Med* 1985;26:1445–1455.
24. Nalcioglu O, Morton ME, Milne N. Computerized longitudinal tomography CLT with a bilateral collimator. *IEEE Trans Nucl Sci* 1980;27:430–434.
25. Myers MJ, Busemann Sokole E, de Bakker J. A comparison of rotating slant-hole collimator and rotating camera for single-photon emission computed tomography of the heart. *Phys Med Biol* 1983;28:581–588.
26. Condon B, Mills J, Ardley R, Taylor D. A physical comparison of two fixed-angle emission tomographic cardiac imaging systems. *Phys Med Biol* 1983;28:131–138.